

time of 12 h. At this resolution, individual VCD features with the same contours as the absorption bands are observed for all the modes. At 4-cm<sup>-1</sup> resolution, band contours for the more isolated bands were reproduced, but the individual contributions from the three modes near 1050 cm<sup>-1</sup> were not resolved. However, the signal-to-noise ratio was considerably higher at the lower resolution (6144 AC and 384 DC scans for each enantiomer). The signs of the VCD intensities calculated by Lowe et al. agree with the experimental observations at 1-cm<sup>-1</sup> resolution. In particular, the VCD couplets due to the modes at 1356 (A), 1300 (B) cm<sup>-1</sup>, and at 1141 (B), 1061 (A) cm<sup>-1</sup> are prominent in both the experiment and calculation.

**Acknowledgment.** This work was supported by grants from the National Science Foundation (CHE 86-02854 to L.A.N. and T.B.F. and CHE 87-21656 to J.E.B.).

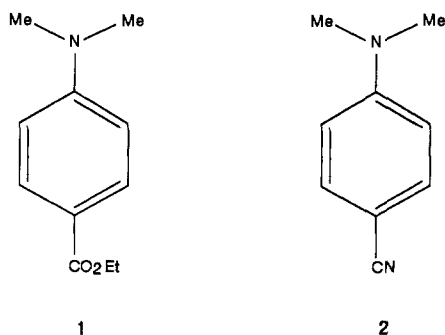
### TICT Fluorescence Emission Dependence on Excitation Wavelength for Ethyl *p*-(Dimethylamino)benzoate in Supercritical Trifluoromethane

Bruce J. Hrnjez,<sup>1</sup> Parvin T. Yazdi,<sup>2</sup> Marye Anne Fox,\*<sup>1</sup> and Keith P. Johnston\*<sup>2</sup>

Departments of Chemistry and Chemical Engineering  
The University of Texas at Austin  
Austin, Texas 78712

Received September 1, 1988

Supercritical fluids<sup>3,4</sup> have only recently been recognized<sup>5,6</sup> for their utility in probing solvent effects on photophysical phenomena. The alluring feature of a supercritical fluid is that a minor perturbation, such as a small change in pressure in the vicinity of the critical point, affords a large change in the density-dependent bulk solvent properties such as dielectric constant and viscosity. Uniquely, then, solvent effects can be probed without change of solvent. We report here the use of supercritical media to examine the highly polarity-dependent formation of the twisted-intramolecular-charge-transfer (TICT)<sup>7</sup> state of ethyl *p*-(dimethylamino)benzoate (**1**).



- (1) Department of Chemistry.
- (2) Department of Chemical Engineering.
- (3) McHugh, M.; Krukonis, V. *Supercritical Fluid Extraction*; Butterworths: Boston, 1986.
- (4) Moore, W. J. *Physical Chemistry*; Prentice-Hall, Inc.: Englewood Cliffs, NJ, 1972; pp 23-25.
- (5) Okada, T.; Kobayashi, Y.; Yamasa, H.; Mataga, N. *Chem. Phys. Lett.* **1986**, *128*, 583.
- (6) Kajimoto, O.; Futakami, M.; Kobayashi, T.; Yamasaki, K. *J. Phys. Chem.* **1988**, *92*, 1347. Kajimoto demonstrated that the fluorescence and absorbance behavior of *p*-(dimethylamino)benzonitrile (**2**) is a useful probe of solute-solvent clustering in supercritical CHF<sub>3</sub>. The use of the supercritical medium as a probe of TICT photophysical behavior was a secondary concern. Johnston previously demonstrated, both experimentally and theoretically, that UV absorbance is a very effective tool for examining solute-solvent interactions in supercritical media. See: Kim, S.; Johnston, K. P. *Ind. Eng. Chem. Res.* **1987**, *26*, 1206.
- (7) Rettig, W. *Angew. Chem., Int. Ed. Engl.* **1986**, *25*, 971.

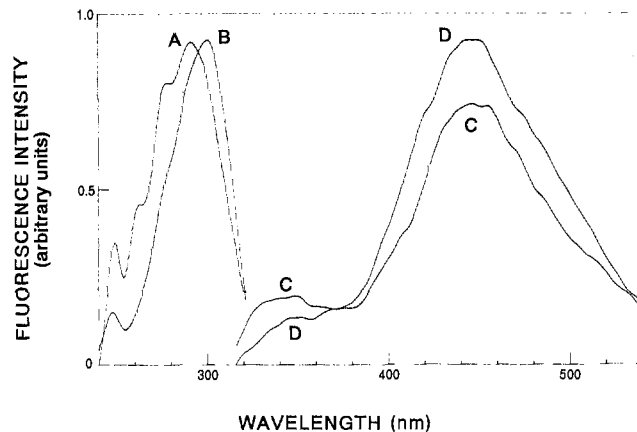


**Figure 1.** Luminescence dependence on excitation wavelength for ester **1** (10<sup>-6</sup> M) in CHF<sub>3</sub> at 28 °C and 102.0 bar. Curve A: excitation spectrum monitored at 350 nm; maximum 291 nm. Curve B: excitation spectrum monitored at 434 nm (intensity divided by a factor of five); maximum 300 nm. Curve C: emission spectrum for excitation at 282 nm; maxima 350 and 444 nm. Curve D: emission spectrum for excitation at 298 nm; maximum 446 nm. Curves C and D are corrected for relative absorbance efficiency. Data collected in ratio mode.

We studied the steady-state fluorescence behavior of **1** in CHF<sub>3</sub> (*T*<sub>c</sub> = 25.9 °C, *P*<sub>c</sub> = 46.9 bar) at 28 °C and several pressures ranging from 44.9 to 136.0 bar. The ester **1** was purified by column chromatography and sublimation, and CHF<sub>3</sub> was deoxygenated by freeze-pump-thaw techniques (< 10 ppm O<sub>2</sub>) and freed of weakly fluorescent impurities by passage through an in-line activated carbon filter.

Representatively, Figure 1 depicts the luminescence behavior of ester **1** (10<sup>-6</sup> M) in CHF<sub>3</sub> at 28 °C and 102.0 bar. The emission profile was a strong function of excitation wavelength for all pressures studied at 28 °C. The excitation spectra, monitored at the planar (curve A) and TICT (curve B) emission maxima, were decidedly nonsuperimposable. Excitation at 282 nm enhanced emission from the short wavelength planar state (curve C), whereas excitation at 298 nm enhanced emission from the long wavelength TICT state (curve D). Similar excitation wavelength dependence was observed for ester **1** in CHF<sub>3</sub> at 50 °C but not at 70 °C. Control experiments showed that ester **1** is stable under our experimental conditions.

This dependence was not observed in normal liquid solvents such as *n*-C<sub>6</sub>H<sub>14</sub>, CH<sub>2</sub>Cl<sub>2</sub>, CHCl<sub>3</sub>, and CH<sub>3</sub>CN; nor was it observed in the supercritical media CO<sub>2</sub> (35 °C) and C<sub>2</sub>H<sub>6</sub> (36 °C) at the many pressures examined. The absence of an excitation wavelength dependence under these conditions indicates that the anomalous dependence in CHF<sub>3</sub> was not due to the presence of an impurity in our sample of ester **1**.

Kajimoto<sup>6</sup> did not report emission dependence on excitation wavelength for the closely related *p*-(dimethylamino)benzonitrile (**2**) in supercritical CHF<sub>3</sub> at 50 °C. We confirmed the absence of excitation wavelength dependence for **2** at 50 °C in CHF<sub>3</sub> and further report that this dependence is absent at 28 °C. These experiments indicate that the presence of an excitation wavelength dependence for **1** in CHF<sub>3</sub> is not due to an impurity in CHF<sub>3</sub> and also suggest that the ester functionality in **1** plays a key role in this dependence phenomenon.

The possibility that deposition of microcrystalline **1** on the emission window or aggregation of **1** in solution could account for the observed excitation energy dependence can be discounted. First, windows of dissimilar materials, both quartz and sapphire, gave identical results. Second, our sample-loading technique precluded initial window deposition. Third, ester **1** is substantially more soluble in CHF<sub>3</sub> than in the nonpolar CO<sub>2</sub> and C<sub>2</sub>H<sub>6</sub>. If aggregation or deposition were to occur, it would most likely do so in the solvents in which **1** is less soluble.

Several instances<sup>8-11</sup> of luminescence dependence on excitation

(8) Al-Hassan, K. A.; Azumi, T. *Chem. Phys. Lett.* **1988**, *146*, 121.

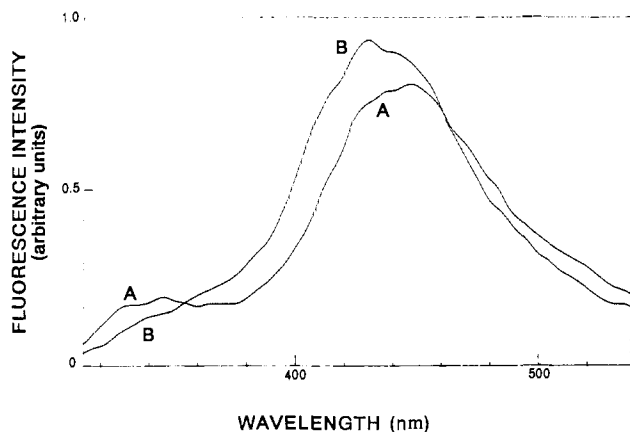


**Figure 2.** Luminescence dependence on pressure for ester **1** ( $10^{-6}$  M) in  $\text{CHF}_3$  at  $28^\circ\text{C}$  with excitation at  $282\text{ nm}$ . Curve A: emission spectrum at  $p = 102.0\text{ bar}$ ; maxima  $350$  and  $446\text{ nm}$ . Curve B: emission spectrum at  $p = 46.3\text{ bar}$ ; maximum  $430\text{ nm}$ . Curves A and B are corrected for changes in relative absorbance efficiency.

energy have been reported. Explanations for these anomalous phenomena generally include factors such as the dependence of intersystem crossing rate on excitation energy, the formation of different solvation sites at low temperatures, and the existence of different conformers in the ground state. Since the  $n\pi^*$  state of the ester **1** is high in energy,<sup>7</sup> it is unlikely that phosphorescence from the triplet can account for our observation that low-energy excitation causes enhanced TICT emission. In rigid media, the existence of different solvation sites or different conformers are satisfactory explanations for the anomalous behavior of closely related TICT-forming systems.<sup>10,11</sup> However, we observed excitation energy dependence in fluid densities of  $\text{CHF}_3$  ranging from gas-like to liquid-like. We suggest that the excitation dependence for **1** in  $\text{CHF}_3$  at  $28^\circ\text{C}$  may be related to differential hydrogen bonding of the ester functionality. An equilibrium distribution of at least two species which differ in the extent to which the ester functionality is hydrogen-bonded would rationalize our observations.

Figure 2 depicts the emission of **1** in  $\text{CHF}_3$  at  $28^\circ\text{C}$  as a function of pressure. An increase in pressure and, therefore, an increase in the dielectric constant of the medium,<sup>3</sup> led to a decrease in the intensity and a red-shift of the long wavelength TICT emission. This was accompanied by an increase in the intensity and no shift in the short wavelength planar emission. Normally, with an increase in solvent polarity the TICT band both shifts to the red and gains in relative intensity.<sup>7</sup> The observed decrease in TICT intensity with increasing pressure suggests that the increase in viscosity of the medium with pressure<sup>3</sup> has an effect on the kinetics of relaxation to the TICT species on the excited-state surface. In fact, this TICT emission intensity dependence on pressure represents further experimental verification of the "twist hypothesis", which dictates hydrodynamic control<sup>7</sup> in the dual fluorescence of **1**.

**Acknowledgment.** We are grateful to the National Science Foundation and the Robert A. Welch Foundation for funding (M.A.F.). Acknowledgment is made to the donors of the Petroleum Research Fund, administered by the American Chemical Society, for partial support of this research (K.P.J.). Preliminary experiments relevant to the spectroscopy reported here were conducted at the Center for Fast Kinetics Research, a facility supported by the National Institutes of Health (RR00886-13) and the University of Texas. We are especially grateful to Dr. E. Kirkov for helpful discussions.

**Registry No. 1,** 10287-53-3;  $\text{CHF}_3$ , 75-46-7.

(9) Al-Hassan, K. A.; El-Bayoumi, M. A. *Chem. Phys. Lett.* **1987**, *138*, 594 and references cited therein.

(10) Dobkowski, J.; Kirkov-Kaminska, E.; Koput, J.; Siemiarczuk, A. *J. Lumin.* **1982**, *27*, 339.

(11) Al-Hassan, K. A.; Rettig, W. *Chem. Phys. Lett.* **1986**, *126*, 273.

## Biosynthesis of Vitamin B<sub>6</sub>: Incorporation of D-1-Deoxyxylulose

Robert E. Hill,<sup>1</sup> Brian G. Sayer,<sup>2</sup> and Ian D. Spenser<sup>\*2</sup>

Departments of Chemistry and Pathology  
McMaster University  
Hamilton, Ontario, Canada, L8S 4M1

Received December 1, 1988

We have shown<sup>3</sup> that the C<sub>8</sub> skeleton of pyridoxol (vitamin B<sub>6</sub>) is derived in toto from the carbon atoms of glucose and, furthermore, that the only two carbon-carbon bonds of the pyridoxol skeleton that are formed de novo in the course of its biosynthesis from glucose are the bonds C-2,3 and C-4,5. This finding confirmed inferences that were drawn from earlier tracer experiments,<sup>4-7</sup> which showed that the C<sub>3</sub> units of pyridoxol, C-3,-4,-4' and C-5',-5,-6, were derived from intact triose phosphate generated from glucose by the normal glycolytic sequence and that the C<sub>2</sub> unit, C-2',-2,-3,-4,-4', of pyridoxol was generated from one such triose phosphate by loss of a terminal carbon atom. We now present evidence that an intact pentose derivative, D-1-deoxyxylulose (**2**), gives rise to the C<sub>5</sub> unit, C-2',-2,-3,-4,-4', of pyridoxol (**3**), i.e., of the unit generated from the C<sub>2</sub> plus one of the C<sub>3</sub> precursors.

In separate experiments cultures of *Escherichia coli* B WG2 were incubated, as described earlier,<sup>4</sup> with D-glucose as the general carbon source, in the presence of D-1-deoxy[1,1,1-<sup>2</sup>H<sub>3</sub>,(RS)-5-<sup>2</sup>H<sub>1</sub>]xylulose<sup>8</sup> (**2**) (experiment 1) and L-1-deoxy[1,1,1-<sup>2</sup>H<sub>3</sub>,(RS)-5-<sup>2</sup>H<sub>1</sub>]xylulose<sup>8</sup> (experiment 2), respectively. Pyridoxol hydrochloride was isolated from each culture after addition of natural abundance pyridoxol hydrochloride (2.5 mg) as carrier and purified by column and thin-layer chromatography, followed by high vacuum sublimation.

The <sup>2</sup>H NMR spectra of the isolated samples of pyridoxol hydrochloride (ca. 1.7 mg in 50  $\mu\text{L}$  of methanol, saturated solution) were recorded on a Bruker AM 500 spectrometer (Figure 1).

The spectra of the two samples (Figure 1 (parts B and D)) were different.

The spectrum of the sample of pyridoxol hydrochloride in methanol, from the *E. coli* B WG2 culture incubated with deuterated L-1-deoxyxylulose (experiment 2) (Figure 1D), was identical with the natural abundance deuterium spectrum of the solvent (Figure 1E). Evidently, deuterium from this substrate had not been incorporated into pyridoxol.

The spectrum of the sample of pyridoxol hydrochloride, obtained from the incubation with deuterium-labeled D-1-deoxyxylulose (experiment 1) (Figure 1B), showed three signals. One of these, at  $\delta$  2.54 ppm, is readily assignable to the C-methyl group, C-2'

(1) Department of Pathology.

(2) Department of Chemistry.

(3) Hill, R. E.; Iwanow, A.; Sayer, B. G.; Wysocka, W.; Spenser, I. D. *J. Biol. Chem.* **1987**, *262*, 7463-7471.

(4) Hill, R. E.; Rowell, F. J.; Gupta, R. N.; Spenser, I. D. *J. Biol. Chem.* **1972**, *247*, 1869-1882.

(5) Hill, R. E.; Horsewood, P.; Spenser, I. D.; Tani, Y. *J. Chem. Soc., Perkin Trans. 1*, **1975**, 1622-1627.

(6) Vella, G. J.; Hill, R. E.; Spenser, I. D. *J. Biol. Chem.* **1981**, *256*, 10469-10474; correction **1982**, *257*, 4008.

(7) Hill, R. E.; Spenser, I. D. In *Vitamin B<sub>6</sub>, Pyridoxal Phosphate; Chemical, Biochemical and Medical Aspects; Part A*; Dolphin, D., Poulson, R., Avramovic, O., Eds.; John Wiley & Sons: New York, 1986; pp 417-476.

(8) D-1-Deoxy[1,1,1-<sup>2</sup>H<sub>3</sub>,(RS)-5-<sup>2</sup>H<sub>1</sub>]xylulose (**2**) was synthesized in six steps from D-arabinose, by a published method.<sup>9</sup> The product **2** was obtained, in the final step of the synthesis, by acid hydrolysis of D-1-deoxy-3,5-O-benzylidene[1,1,1-<sup>2</sup>H<sub>3</sub>,(RS)-5-<sup>2</sup>H<sub>1</sub>]xylulose (**1**), whose purity and deuterium content was determined by <sup>1</sup>H and <sup>2</sup>H NMR spectroscopy: <sup>1</sup>H NMR (CCl<sub>4</sub>)  $\delta$  (ppm) 3.95 (1 H, H-4), 4.06 (0.4 H, H-5 $\beta$ ), 4.20 (0.6 H, H-5 $\alpha$ ), 4.25 (1 H, H-3), 5.60 (1 H, PhCH); <sup>2</sup>H NMR (CCl<sub>4</sub>)  $\delta$  (ppm) 2.26 (3 <sup>2</sup>H, CD<sub>3</sub>), 4.09 (0.61 <sup>2</sup>H, D-5 $\beta$ ), 4.23 (0.43 <sup>2</sup>H, D-5 $\alpha$ ); <sup>2</sup>H content at the C-methyl group 100%; at 5 $\beta$  61%; at 5 $\alpha$  43%; ratio: <sup>2</sup>H at CD<sub>3</sub>/<sup>2</sup>H at (5 $\beta$  plus 5 $\alpha$ ) = 3/(1 + 0.61 + 0.43) = 3:1.04. L-1-Deoxy[1,1,1-<sup>2</sup>H<sub>3</sub>,(RS)-5-<sup>2</sup>H<sub>1</sub>]xylulose was obtained analogously, from L-arabinose. In each of the two experiments, a culture of *E. coli* B WG2 was incubated in the presence of D-glucose as the general carbon source with the deuterium-labeled samples of 1-deoxyxylulose. Expt. 1: D-deoxy[1,1,1-<sup>2</sup>H<sub>3</sub>,(RS)-5-<sup>2</sup>H<sub>1</sub>]xylulose (1 g), D-glucose (1 g). Expt. 2: L-1-deoxy[1,1,1-<sup>2</sup>H<sub>3</sub>,(RS)-5-<sup>2</sup>H<sub>1</sub>]xylulose (0.7 g), D-glucose (0.7 g).